



Removing Noise and Preserving Details with Relaxed Median Filters

ABDESSAMAD BEN HAMZA

Dept. de Matemática Aplicada, Universidad de Granada, Spain

PEDRO L. LUQUE-ESCAMILLA

Dept. de Ingeniería Mecánica y Minera, Universidad de Jaen, Spain

JOSÉ MARTÍNEZ-AROZA

Dept. de Matemática Aplicada, Universidad de Granada, Spain

RAMÓN ROMÁN-ROLDÁN

Dept. de Física Aplicada, Universidad de Granada, Spain

Abstract. In this paper, a median based filter called *relaxed median filter* is proposed. The filter is obtained by relaxing the order statistic for pixel substitution. Noise attenuation properties as well as edge and line preservation are analyzed statistically. The trade-off between noise elimination and detail preservation is widely analyzed. It is shown that relaxed median filters preserve details better than the standard median filter, and remove noise better than other median type filters.

Keywords: median type-filters, statistical properties, nonlinear filtering

1. Introduction

The median filter has been proven to be very useful in many image processing applications. In a median filter, a window slides across the data and the median value of the samples inside the window is chosen to be the output of the filter. This nonlinear filter, compared to linear ones, shows certain advantages: edge preservation and efficient noise attenuation with robustness against impulsive-type noise [1, 2].

In spite of this, the median filter is far from being a perfect filtering method since it may remove fine details, sharp corners and thin lines. The main reason is that the ordering process destroys any structural and spatial neighborhood information [1].

Recently, several versions of the median filter, such as multilevel and multistage filters [3, 4], weighted median filters [5–9], stack filters [10, 11], nested median filters [13], rank conditioned rank selection filters [14] and other median based filters [1], which allow more

flexible trade-off between the image detail preservation and the noise removing, have been developed. In this paper a median based filter called *relaxed median filter* is introduced, having similar properties as the above mentioned filters, while being simpler and easier to implement than them.

The paper is organized as follows. In Section 2, we define the relaxed median filter. In Section 3, the statistical behavior of the relaxed median filter is studied. Some experimental results are presented in Section 4 and, finally, Section 5 gives some conclusions.

2. Relaxed Median Filters

Let $\{X_i\}$ be a m -dimensional sequence, where the index $\mathbf{i} \in \mathbb{Z}^m$. A sliding window is defined as a subset $W \subset \mathbb{Z}^m$ of odd size $2N + 1$. Given a sliding window W , define $W_i = \{X_{\mathbf{i}+\mathbf{r}}: \mathbf{r} \in W\}$ to be the window located at position \mathbf{i} .

If we let X_i and Y_i be the input and the output at location \mathbf{i} , respectively, of the filter, then we have for the standard median (SM) filter:

$$Y_i = \text{med}\{W_i\} = \text{med}\{X_{i+r} : \mathbf{r} \in W\},$$

where $\text{med}\{\cdot\}$ denotes the median operator.

Denote by $[W_i]_{(r)}$, $r = 1, \dots, 2N + 1$, the r th order statistic of the samples inside the window W_i :

$$[W_i]_{(1)} \leq [W_i]_{(2)} \leq \dots \leq [W_i]_{(2N+1)}.$$

The relaxed median filter works as follows: two bounds ℓ and u —lower and upper, respectively—define a sublist inside the $[W_i]_{(\cdot)}$, which contains the gray levels that we assume to be good enough not to be filtered.

If the input belongs to the sublist, then it remains unfiltered, otherwise the standard median filter is output.

Definition 1. Let $m = N + 1$ and ℓ, u such that $1 \leq \ell \leq m \leq u \leq 2N + 1$. The relaxed median filter with bounds ℓ and u is defined as

$$Y_i = \text{RM}_{\ell u}\{W_i\} = \begin{cases} X_i & \text{if } X_i \in [[W_i]_{(\ell)}, [W_i]_{(u)}] \\ [W_i]_{(m)} & \text{otherwise} \end{cases}$$

where $[W_i]_{(m)}$ is the median value of the samples inside the window W_i .

As it can be easily seen, this new filter is at least as fast as the center weighted median filter, but slightly slower than the standard median filter.

It is worth noticing that the symmetric relaxed median filter (i.e. in the case where $\ell = 2N + 2 - u$) is the same as the rank conditioned median filter which is a subclass of RCRC filters [14]. In this paper, the output distribution of the relaxed median filter is given for a more generalized form, and the statistical properties of detail preservation are also presented and illustrated.

3. Statistical Properties of Relaxed Median Filters

The performance of the relaxed median filter should be described by using some statistics of the output. However, this is not possible in general since accurate statistical descriptions of input images are difficult to obtain. But it is still possible to obtain the probability distribution function of the output by making simple assumptions about the original image (before being

corrupted by noise). In this sense, the noise attenuation can be well assessed from homogeneous originals and the detail preservation can be assessed from pure edges and lines.

3.1. Output Distribution

In this section, the output distribution of relaxed median filters is derived from an homogeneous original.

Theorem 1. Let the input of a relaxed median filter, with window size $2N + 1$, be i.i.d. with a distribution function $\Phi(t)$. The distribution function $\Psi(t)$ of the output is given by

$$\begin{aligned} \Psi(t) = & \sum_{k=m-1}^{2N} \binom{2N}{k} \Phi(t)^{k+1} (1 - \Phi(t))^{2N-k} \\ & + \sum_{k=\ell-1}^{m-2} \frac{k - \ell + 2}{k + 1} \binom{2N}{k} \\ & \times \Phi(t)^{k+1} (1 - \Phi(t))^{2N-k} \\ & + \sum_{k=u}^{2N} \sum_{k'=m}^k \frac{1}{2N + 1 - k'} \binom{2N}{k'} \\ & \times \Phi(t)^{k'} (1 - \Phi(t))^{2N+1-k'} \end{aligned} \quad (1)$$

where ℓ and u are such that $1 \leq \ell \leq m \leq u \leq 2N + 1$.

Proof: See the Appendix. \square

3.2. Output Moments

From the output distribution of relaxed median filters, we can derive the moments of relaxed median filters.

Let the input values X_i be independent, identically distributed random variables having a distribution function $\Phi(t)$.

For $r \leq s$ and $\alpha \in \mathbb{N}$, define

$$V_r(s, \Phi, \alpha) = \int_{-\infty}^{+\infty} t^\alpha \frac{d}{dt} (\Phi(t)^r (1 - \Phi(t))^{s-r}) dt.$$

It is straightforward to obtain the following theorem according to the definition of the moments.

Theorem 2. Given a relaxed median filter with window size $2N + 1$, for i.i.d. input with distribution

function $\Phi(t)$, the α -order moments, denoted by m_α , of the output are given by

$$\begin{aligned}
 m_\alpha &= \sum_{k=m-1}^{2N} \binom{2N}{k} V_{k+1}(2N+1, \Phi, \alpha) \\
 &+ \sum_{k=\ell-1}^{m-2} \frac{k-\ell+2}{k+1} \binom{2N}{k} \\
 &\times V_{k+1}(2N+1, \Phi, \alpha) \\
 &+ \sum_{k=u}^{2N} \sum_{k'=m}^k \frac{1}{2N+1-k'} \binom{2N}{k'} \\
 &\times V_{k'}(2N+1, \Phi, \alpha). \tag{2}
 \end{aligned}$$

Furthermore, if for $r \leq s$ and $\alpha \in \mathbb{N}$ we define

$$\begin{aligned}
 W_r(s, \Phi, \alpha) \\
 = \int_{-\infty}^{+\infty} (t-m^1)^\alpha \frac{d}{dt} (\Phi(t)^r (1-\Phi(t))^{s-r}) dt,
 \end{aligned}$$

then the α -order central moments, denoted by μ_α , of the output can be expressed as

$$\begin{aligned}
 \mu_\alpha &= \sum_{k=m-1}^{2N} \binom{2N}{k} W_{k+1}(2N+1, \Phi, \alpha) \\
 &+ \sum_{k=\ell-1}^{m-2} \frac{k-\ell+2}{k+1} \binom{2N}{k} \\
 &\times W_{k+1}(2N+1, \Phi, \alpha) \\
 &+ \sum_{k=u}^{2N} \sum_{k'=m}^k \frac{1}{2N+1-k'} \\
 &\times \binom{2N}{k'} W_{k'}(2N+1, \Phi, \alpha). \tag{3}
 \end{aligned}$$

3.3. Additive White Noise Suppression

Using Theorem 2, we can compute the variance (2-order output central moment) of relaxed median filters, for various values of ℓ and u , through numerical integration for i.i.d. inputs with a given distribution function $\Phi(t)$.

In order to compare the performance of relaxed median filters with some other median based filters in eliminating Gaussian white noise, here we briefly review

some statistical properties of weighted median (WM) filters.

The output Y_i of the WM filter with weight set $\Omega = (\omega_r)$ is given by

$$Y_i = \text{med}\{\omega_r \diamond X_{i+r}; r \in W\}$$

where \diamond denotes duplication:

$$\omega \diamond x = \overbrace{x, \dots, x}^{\omega \text{ times}}.$$

Here a theorem from [9] is given for self-containment.

Theorem 3. *Let the inputs of a WM filter, with window size $2N+1$, be i.i.d. with a distribution function $\Phi(t)$. The output distribution of the WM filter Ψ_{wm} has the following form:*

$$\begin{aligned}
 \Psi_{\text{wm}}(t) &= \Psi_{\text{med}}(t) + \sum_{k=1}^N M_k [\Phi(t)^k (1-\Phi(t))^{2N+1-k} \\
 &- \Phi(t)^{2N+1-k} (1-\Phi(t))^k] \tag{4}
 \end{aligned}$$

where $\Psi_{\text{med}}(t)$ is the output distribution of the standard median filter with the same window size and M_k 's represent the number of different weight combinations, in which there are k weights and the sum of these k weights is larger than or equal to a threshold T .

Furthermore, the output variance of this window size $2N+1$ WM filter can be expressed as:

$$\sigma_{\text{wm}}^2 = \sigma_{\text{med}}^2 + \sum_{k=1}^N M_k L_k(2N+1, \Phi) \tag{5}$$

where σ_{med}^2 is the output variance of the window size $2N+1$ standard median filter and

$$L_k(2N+1, \Phi) = \int_{-\infty}^{+\infty} G_k(2N+1, \Phi) t^2 d\Phi(t)$$

being

$$\begin{aligned}
 G_k(2N+1, \Phi) \\
 &= (k - (2N+1)\Phi(t))\Phi(t)^{k-1}(1-\Phi(t))^{2N-k} \\
 &+ (k - (2N+1)(1-\Phi(t)))\Phi(t)^{2N-k} \\
 &\times (1-\Phi(t))^{k-1}.
 \end{aligned}$$

Based on the above result, let us study the following WM filter

$$\mathcal{W} = \begin{pmatrix} \omega & \omega & \omega \\ \omega & \omega_0 & \omega \\ \omega & \omega & \omega \end{pmatrix},$$

with $\omega \geq 2$ and such that $8\omega + \omega_0$ is an odd number. Its threshold is $T = \frac{1}{2}(8\omega + \omega_0 + 1)$. Two cases are distinguished:

- (1) $3\omega + \omega_0 < T$ i.e. $\omega_0 < 2\omega + 1$. Denote this WM filter by $\text{WM}_{3 \times 3}^{(1)}$. It is obvious to find that

$$M_k = 0 \quad k = 1, \dots, 4.$$

Hence, $\sigma_{\text{wm}}^2 = \sigma_{\text{med}}^2 \approx 0.166$ when the input is i.i.d. $\mathcal{N}(0, 1)$. That is, this weighted median filter and the standard median filter, with the same window size 3×3 , perform equal in removing additive white Gaussian noise, and better than a relaxed median filter $\text{RM}_{4,6}$ with the same window size.

- (2) $3\omega + \omega_0 \geq T$ i.e. $\omega_0 \geq 2\omega + 1$. Denote this WM filter by $\text{WM}_{3 \times 3}^{(2)}$. It is easy to find that

$$M_k = 0 \quad k = 1, \dots, 3 \quad \text{and} \quad M_4 = 56.$$

Then, $\sigma_{\text{wm}}^2 = \sigma_{\text{med}}^2 + M_4 L_4(9, \Phi) \approx 0.237$ when the input is i.i.d. $\mathcal{N}(0, 1)$. That is, this weighted median filter performs worse than a relaxed median filter $\text{RM}_{4,6}$, with the same window size, in suppressing additive white Gaussian noise.

Table 1 shows the output variances of relaxed median filters and the weighted median filter $\text{WM}_{3 \times 3}^{(2)}$ for i.i.d inputs of the three commonly used noise distributions,

Table 1. Output variances of relaxed median and $\text{WM}_{3 \times 3}^{(2)}$ filters for i.i.d. inputs $\mathcal{N}(0, 1)$, $\mathcal{L}(0, 1)$ and $\mathcal{U}(0, 1)$ with window size 3×3 .

Filter type (3×3)	Variance		
	$\mathcal{N}(0, 1)$	$\mathcal{L}(0, 1)$	$\mathcal{U}(0, 1)$
$\text{RM}_{2,8}$	0.467	0.341	0.612
$\text{RM}_{3,7}$	0.261	0.157	0.393
$\text{WM}_{3 \times 3}^{(2)}$	0.237	0.135	0.369
$\text{RM}_{4,6}$	0.183	0.099	0.296
$\text{RM}_{5,5} = \text{SM}$	0.166	0.087	0.272

Normal, Laplace and Uniform with zero mean and unit variance, denoted by $\mathcal{N}(0, 1)$, $\mathcal{L}(0, 1)$ and $\mathcal{U}(0, 1)$, respectively. With the aid of this table, one can easily compare the noise attenuation capability of different relaxed median filters. It can be seen that the variance of the relaxed median filter is greater than that of the standard median filter. Furthermore, we observe that the $\text{RM}_{4,6}$ filter performs better than the $\text{WM}_{3 \times 3}^{(2)}$ filter in eliminating the additive white noise.

3.4. Impulsive Noise Filtering

In impulsive noise environments, if there are several noisy samples clustered together, impulses may not be removed from the image. It is very helpful to quantify the probability of such an event. As defined in [4], the *breakdown probability* is the probability of an impulse occurring at the output of the filter, and relating it to the corresponding probability p of impulses at the input, is useful to assess the robustness of the filter. The breakdown probability, in homogeneous originals, follows from Theorem 1.

Theorem 4. Given a relaxed median filter with window size $2N + 1$, the breakdown probability, denoted by $B(p)$, of the relaxed median filter is given by

$$\begin{aligned} B(p) = & \sum_{k=m-1}^{2N} \binom{2N}{k} p^{k+1} (1-p)^{2N-k} \\ & + \sum_{k=\ell-1}^{m-2} \frac{k-\ell+2}{k+1} \binom{2N}{k} p^{k+1} (1-p)^{2N-k} \\ & + \sum_{k=u}^{2N} \sum_{k'=m}^k \frac{1}{2N+1-k'} \binom{2N}{k'} \\ & \times p^{k'} (1-p)^{2N+1-k'}. \end{aligned} \quad (6)$$

Figure 1 shows plots of breakdown probabilities of (a) a relaxed median filter $\text{RM}_{4,6}$ with the window size 3×3 , (b) a standard median filter (SM) with the same window size and (c) a weighted median filter $\text{WM}_{3 \times 3}^{(2)}$. In Fig. 1(d) the solid curve plots the difference between breakdown probabilities of $\text{RM}_{4,6}$ and $\text{RM}_{5,5}$ while the dashed curve is corresponding to the difference between breakdown probabilities of $\text{WM}_{3 \times 3}^{(2)}$ and $\text{RM}_{4,6}$. From this figure, we deduce that for small probabilities of impulses the $\text{RM}_{4,6}$ filter occupies an intermediate position in attenuating the impulsive noise.

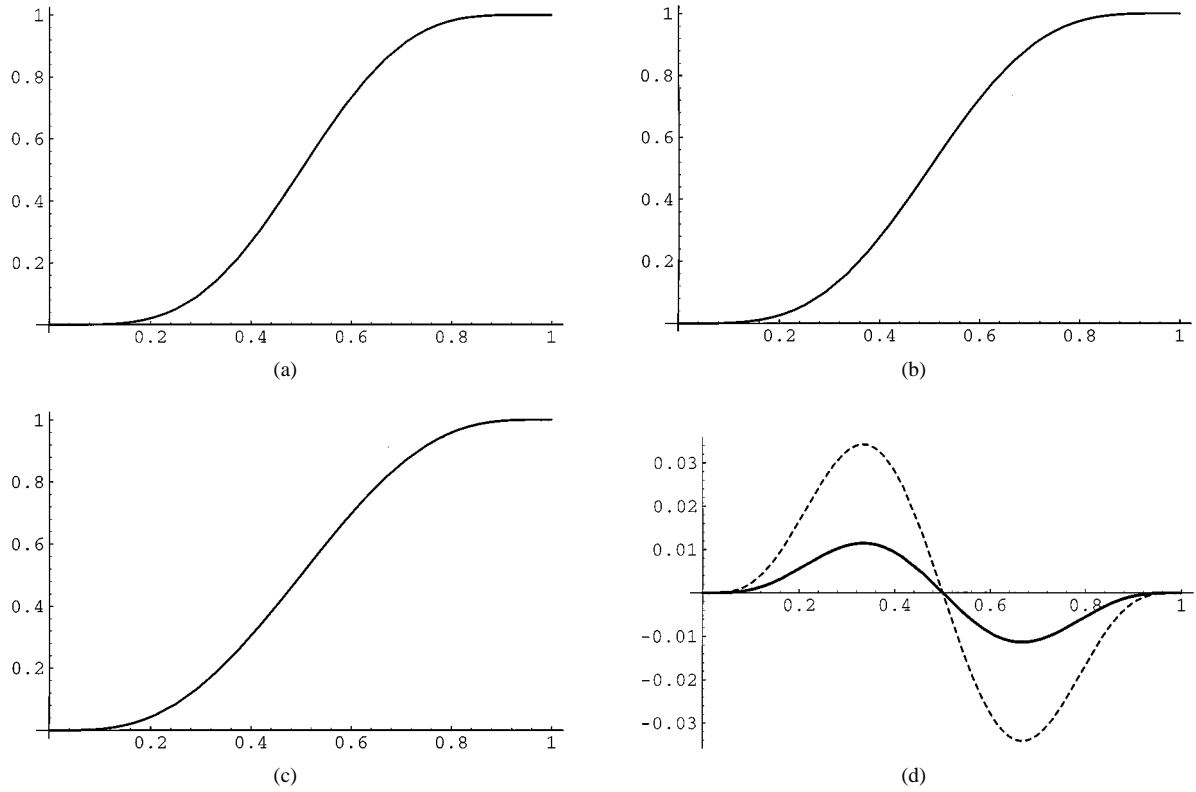


Figure 1. Breakdown probabilities of (a) a relaxed median filter $RM_{4,6}$ with the window size 3×3 , (b) standard median filter $RM_{5,5} = SM$ with the same window size and (c) a weighted median filter $WM_{3 \times 3}^{(2)}$. In (d) the solid (resp. the dashed) curve corresponds to the difference between breakdown probabilities of $RM_{4,6}$ and $RM_{5,5}$ (resp. of $WM_{3 \times 3}^{(2)}$ and $RM_{4,6}$).

3.5. Edge Preservation in the Presence of Additive White Noise

The effects of relaxed median filters on noisy step edges are considered now. Start by defining the noisy step edge image X_{ij} given by

$$X_{ij} = \begin{cases} v_{ij} & \text{if } (i, j) \in A \\ h + v_{ij} & \text{if } (i, j) \in B, \end{cases} \quad (7)$$

where $A = \{(i, j) \mid j > 0\}$ and $B = \{(i, j) \mid j \leq 0\}$ denote, respectively, the upper and the lower part of the step edge, h is a constant representing the step height, and v_{ij} is i.i.d. noise.

Denote by $\Phi_A(t)$ and $\Phi_B(t) = \Phi_A(t - h)$ the distribution functions of the samples located in A and B respectively.

The filter behavior in the vicinity of the noisy edge is going to be examined by computing $E(Y_{ij})$, $\text{Var}(Y_{ij})$ and the root mean square error $\text{rmse}(i, j) =$

$\sqrt{E(Y_{ij} - S_{ij})^2}$ where Y_{ij} is the filtered image and S_{ij} is given by $S_{ij} = \begin{cases} 0 & \text{if } (i, j) \in A \\ h & \text{if } (i, j) \in B. \end{cases}$ Denote by m_{ij} the number of samples of the window located in A . This number depends on the location of the window W_{ij} , and the number of samples located in B is $2N + 1 - m_{ij}$.

The next result will allow us to assess the edge preservation.

Theorem 5. For the noisy step edge input in (7), the output distribution function $\Psi_{Y_{ij}}(t)$ of the relaxed median filter with window size $2N + 1$ is given by

$$\begin{aligned} \Psi_{Y_{ij}}(t) = & \sum_{k=m-1}^{2N} \sum_{n_0=\max\{0, k-(2N-d_{ij})\}}^{\min\{k, d_{ij}\}} \binom{d_{ij}}{n_0} \binom{2N-d_{ij}}{k-n_0} \\ & \times \Phi_A(t)^{n_0} (1 - \Phi_A(t))^{d_{ij}-n_0} \times \Phi_B(t)^{k-n_0} \\ & \times (1 - \Phi_B(t))^{2N-d_{ij}-k+n_0} \times \Phi_{ij}(t) \end{aligned}$$

$$\begin{aligned}
 & + \sum_{k=\ell-1}^{m-2} \sum_{n_0=\max\{0, k-(2N-d_{ij})\}}^{\min\{k, d_{ij}\}} \binom{d_{ij}}{n_0} \\
 & \times \binom{2N-d_{ij}}{k-n_0} \frac{k-\ell+2}{k+1} \\
 & \times \Phi_A(t)^{n_0} (1-\Phi_A(t))^{d_{ij}-n_0} \times \Phi_B(t)^{k-n_0} \\
 & \times (1-\Phi_B(t))^{2N-d_{ij}-k+n_0} \times \Phi_{ij}(t) \\
 & + \sum_{k=u}^{2N} \sum_{k'=m}^k \sum_{n_0=\max\{0, k'-(2N-d_{ij})\}}^{\min\{k', d_{ij}\}} \binom{d_{ij}}{n_0} \\
 & \times \binom{2N-d_{ij}}{k'-n_0} \frac{1}{2N+1-k'} \\
 & \times \Phi_A(t)^{n_0} (1-\Phi_A(t))^{d_{ij}-n_0} \times \Phi_B(t)^{k'-n_0} \\
 & \times (1-\Phi_B(t))^{2N-d_{ij}-k'+n_0} \times (1-\Phi_{ij}(t))
 \end{aligned} \tag{8}$$

where

$$\Phi_{ij}(t) = \begin{cases} \Phi_A(t) & \text{if } (i, j) \in A \\ \Phi_B(t) & \text{if } (i, j) \in B \end{cases}$$

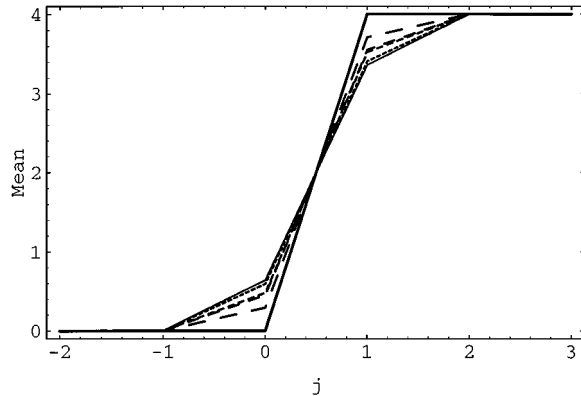
and

$$d_{ij} = \begin{cases} m_{ij} - 1 & \text{if } (i, j) \in A \\ m_{ij} & \text{if } (i, j) \in B. \end{cases}$$

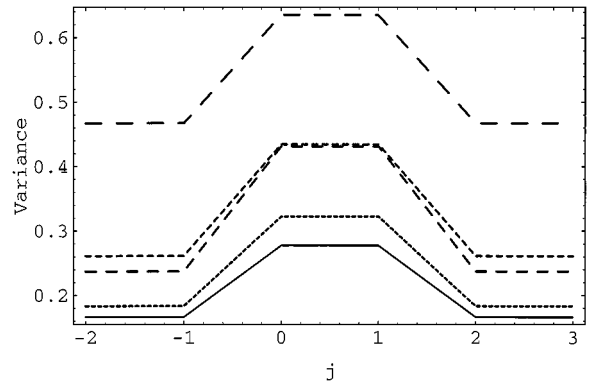
Proof: See the Appendix. \square

Using Theorem 5, we can compute $E(Y_{ij})$, $\text{Var}(Y_{ij})$ and the root mean square error $\text{rmse}(i, j)$ of relaxed median filters with a given distribution function $\Phi_A(t)$ through numerical integration with i fixed, j variable and a given value of h . As an example of application, we suppose that Φ_A is $\mathcal{N}(0, 1)$.

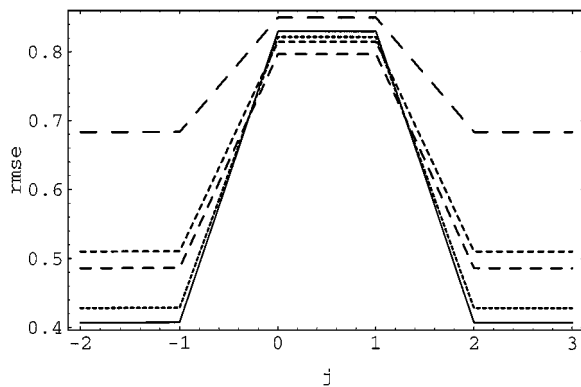
Figure 2 shows plots of mean, variance and rmse for relaxed median filters and center weighted median filter with a 3×3 square window, when a step edge with $h = 4$ is degraded by a Gaussian noise $\mathcal{N}(0, 1)$.



(a)



(b)



(c)

- RM_{2,8}
- .-.- RM_{3,7}
- ... CWM(2K + 1 = 3)
- RM_{4,6}
- RM_{5,5} = SM
- Step edge

Figure 2. Results of relaxed median filters and a CWM(2K + 1 = 3) filter, with 3×3 square window, for the noisy step edge $h = 4$. (a) The mean. (b) The variance. (c) The rmse.

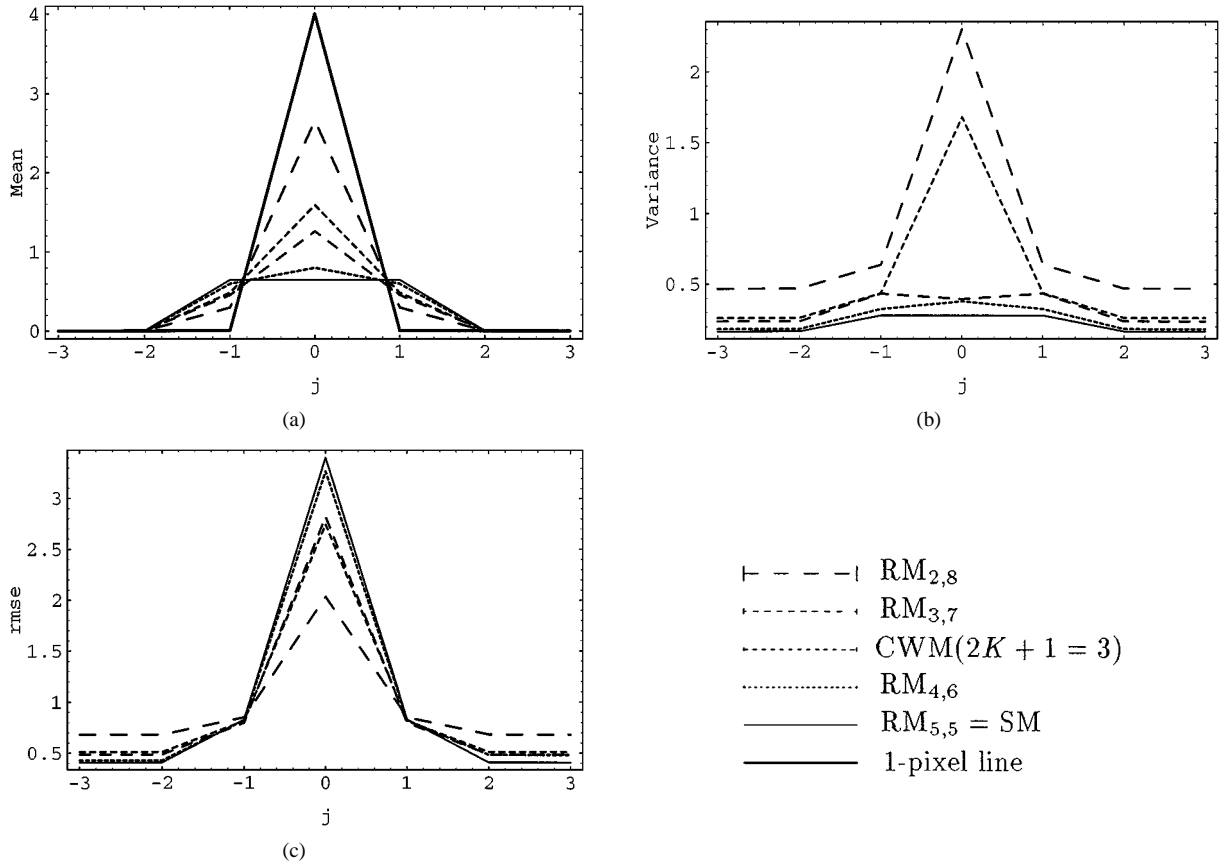


Figure 3. Results of relaxed median filters and a CWM($2K + 2 = 3$) filter, with 3×3 square window, for the one pixel wide noisy line $h = 4$. (a) The mean. (b) The variance. (c) The rmse.

The results show that relaxed median filters do preserve edges better than standard median filter, as expected.

3.6. Line Preservation in the Presence of Additive White Noise

Consider the k -pixel wide noisy line image X_{ij} expressed as

$$X_{ij} = \begin{cases} v_{ij} & \text{if } (i, j) \in A \\ h + v_{ij} & \text{if } (i, j) \in B \end{cases} \quad (9)$$

where $A = \{(i, j) \mid j \neq 0, 1, \dots, k-1\}$ and $B = \{(i, j) \mid j = 0, 1, \dots, k-1\}$ denote, respectively, the locations outside the line and inside it, h is a constant representing the line height, and v_{ij} is i.i.d. noise with distribution function $\Phi_A(t)$.

Theorem 6. For the noisy line input in (9), the output distribution function $\Psi_{Y_{ij}}(t)$ of the relaxed median filter with window size $2N + 1$ has the same expression (8)

as in the case of the step edge (Theorem 5) except for the definitions of A and B .

Theorem 6 is applied to compute $E(Y_{ij})$, $\text{Var}(Y_{ij})$ and the root mean square error $\text{rmse}(i, j)$ of relaxed median filters with a given distribution function $\Phi_A(t)$ through numerical integration with i fixed, j variable and a given value of h . Suppose that the lines are corrupted by Gaussian noise i.e. Φ_A is $\mathcal{N}(0, 1)$.

Figures 3 and 4 show plots of mean, variance and rmse for relaxed median filters and a CWM($2K + 1 = 3$) filter with a 3×3 for the 1-pixel wide noisy line and 2-pixel wide noisy line respectively, with $h = 4$. It is clear to see that relaxed median filters show a good line preservation.

4. Experimental Results

This section presents experimental results where relaxed median filters are applied to enhance images corrupted by additive white noise or impulsive noise.

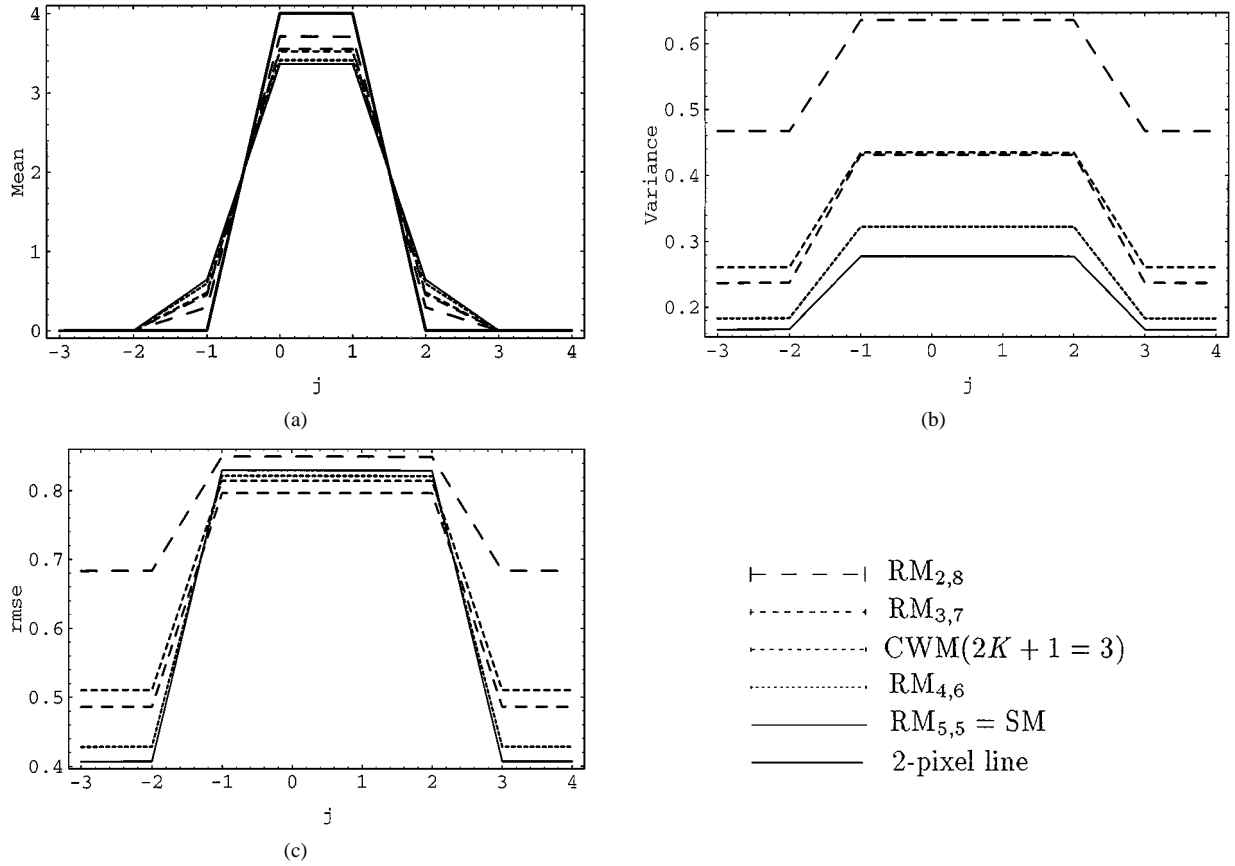


Figure 4. Results of relaxed median filters and a CWM(2K + 1 = 3) filter, with 3 × 3 square window, for the two pixel wide noisy line h = 4. (a) The mean. (b) The variance. (c) The rmse.

Normalized mean absolute error (NMAE) between the original image and the filtered image is evaluated to quantitatively compare the performance of the relaxed median filters presented in this paper to that of other filters [7, 8]. The NMAE is defined as

$$\text{NMAE} = \frac{\sum_i \sum_j |Y_{ij} - S_{ij}|}{\sum_i \sum_j |X_{ij} - S_{ij}|}$$

where S_{ij} , X_{ij} and Y_{ij} are the original, noisy and filtered images, respectively.

4.1. Additive White Noise Attenuation

Figure 5(a) shows the original image which consists of 256 × 256 pixels with 8-bit of resolution. Three noisy images were generated by adding zero mean i.i.d. Gaussian noise of variance 200, 400 and 625 to the original image, and were then filtered by various median

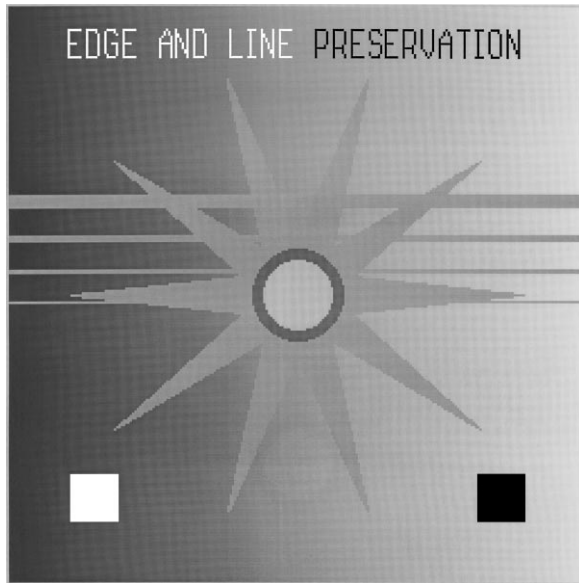
based filters with a 3 × 3 square window. The noisy image with noise variance 200 is shown in Fig. 5(b).

Table 2 shows the NMAE's of a standard median (SM), a relaxed median (RM_{4,6}) and a center weighted median CWM(2K + 1 = 3) [7, 8].

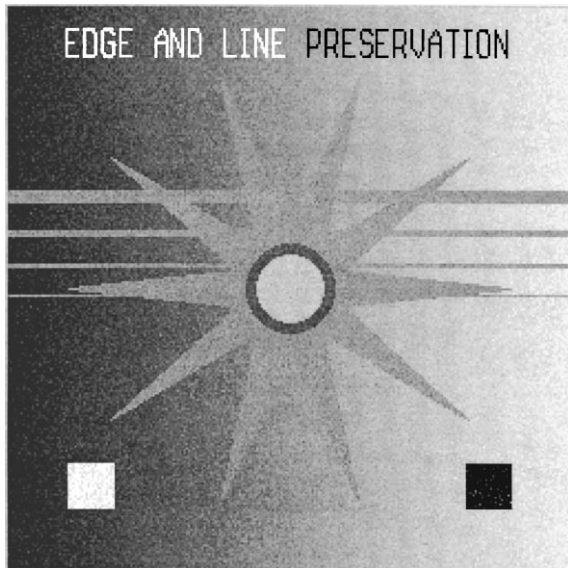
Figure 6 shows the results of filtering the noisy image in Fig. 5(b) by a standard median filter (SM), a relaxed median filter (RM_{4,6}) and a center weighted median filter CWM(2K + 1 = 3). As shown in the images, a RM_{4,6} filter preserves more details than a SM filter,

Table 2. NMAE's results for additive white Gaussian noise.

Filter type (3 × 3)	NMAE		
	$\sigma^2 = 200$	$\sigma^2 = 400$	$\sigma^2 = 625$
CWM(2K + 1 = 3)	0.671385	0.622358	0.604413
RM _{4,6}	0.661933	0.616405	0.591093
RM _{5,5} = SM	0.660175	0.602671	0.574727



(a)



(b)

Figure 5. (a) Original image. (b) Noisy image corrupted by Gaussian noise ($\sigma^2 = 200$).

and still gives a good noise attenuation with respect to a $CWM(2K + 1 = 3)$ filter.

4.2. Impulsive Noise Filtering

It is well known that median based filters are effective and better than linear filters, in general, in removing im-

Table 3. NMAE's results for impulsive noise.

Filter type (3×3)	NMAE		
	$p = 0.1$	$p = 0.15$	$p = 0.3$
$CWM(2K + 1 = 3)$	0.152806	0.129732	0.189396
$RM_{4,6}$	0.145936	0.128888	0.180551
$RM_{5,5} = SM$	0.201959	0.157360	0.139182

Table 4. NMAE's results for impulsive noise.

Filter type (3×3)	NMAE		
	$p = 0.1$	$p = 0.15$	$p = 0.3$
$CWM(2K + 1 = 3)$	0.262925	0.209358	0.229586
$RM_{4,6}$	0.315791	0.239451	0.246328
$RM_{5,5} = SM$	0.412596	0.293025	0.210835

pulsive noise. The noisy image in Fig. 7(b) is corrupted by both positive and negative impulses having values 255 and 0. Three images were generated by considering three probabilities of impulses $p = 0.1, 0.15$, and 0.3 . Figure 7(b) shows a noisy image corrupted by impulsive noise ($p = 0.1$).

The NMAE's results of the filters are shown in Table 3. Figure 8 shows the results of filtering the noisy image in Fig. 7(b) by a standard median filter, a relaxed median filter ($RM_{4,6}$) and a center weighted median filter $CWM(2K + 1 = 3)$. Comparison of these images clearly indicates that a $RM_{4,6}$ filter preserves details while also suppressing impulses.

Figure 9(b) shows a noisy image corrupted by impulsive noise ($p = 0.15$). The NMAE's results of the filters are shown in Table 4. Figure 10 shows the results of filtering the noisy image in Fig. 9(b) by a standard median filter, a relaxed median filter ($RM_{4,6}$) and a center weighted median filter $CWM(2K + 1 = 3)$. Comparison of these images clearly indicates that a $RM_{4,6}$ filter preserves details while also suppressing impulses.

5. Conclusions

In this paper, relaxed median filters were proposed. The behavior and performance of relaxed median filters are assessed using their statistical properties. Both noise elimination and detail preservation have been discussed.

By using the expression of the output distribution of relaxed median filters, other statistical properties have been derived.

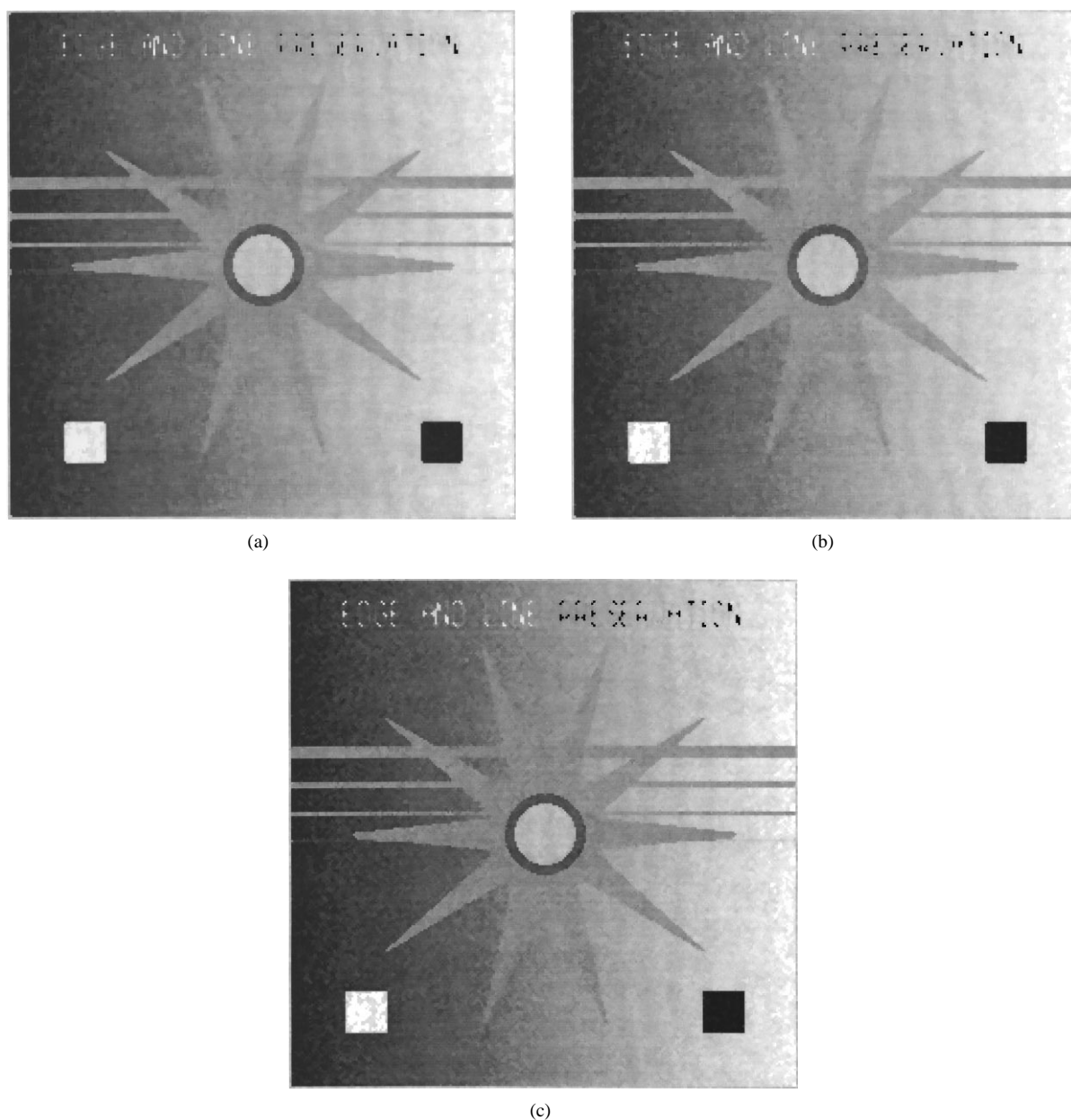


Figure 6. The results of the filtered noisy image in Fig. 5(b) with a 3×3 square window by (a) a median filter (SM), (b) a relaxed median filter ($RM_{4,6}$) and (c) a center weighted median filter $CWM(2K + 1 = 3)$.

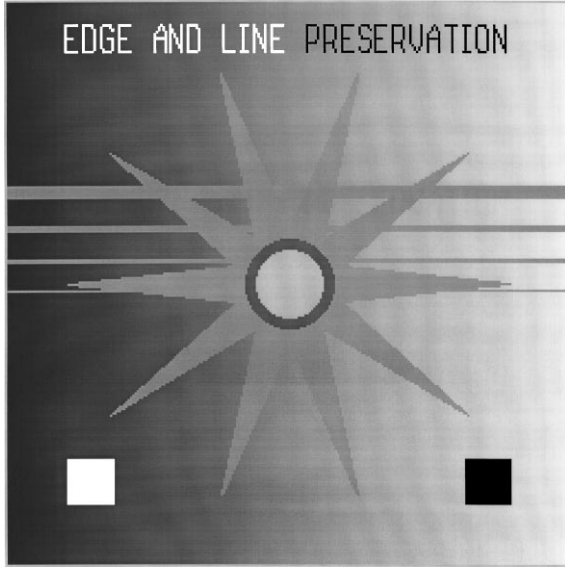
It was shown that there exists a clear trade-off between detail preservation and noise suppression properties of the relaxed median filter, and the longer the upper bound of this filter, the better noise attenuation ability the filter has.

The main properties of the filters and simulation results are given, showing the improvement in preserving details with respect to the standard median filter, and

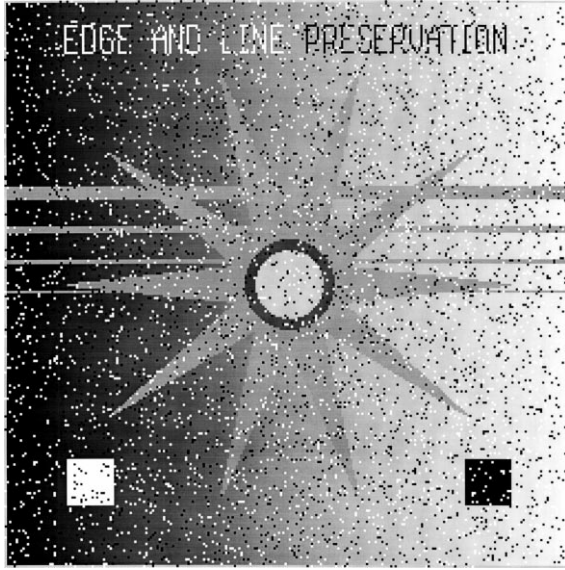
in removing noise with respect to other median based filters.

Appendix

In this appendix, proofs of theorems are given. First, we briefly review some properties of order statistics [12]



(a)



(b)

Figure 7. (a) Original image. (b) Noisy image corrupted by impulsive noise 10%.

that will be used in the statistical analysis of relaxed median filters.

Theorem 7. Suppose that X_i are independent and identically distributed (i.i.d.) random variables, each with distribution function $\Phi(t)$. Let $\Phi_r(t)$ denote the distribution function of the r th order statistic

$[W_i]_{(r)}$, $r = 1, \dots, 2N + 1$. Then

$$\begin{aligned} \Phi_r(t) &= \Pr[W_i]_{(r)} \leq t \\ &= \sum_{k=r}^{2N+1} \binom{2N+1}{k} \Phi(t)^k (1 - \Phi(t))^{2N+1-k}. \end{aligned}$$

Theorem 8. For $t' < t$, the joint distribution function $\Phi_{r,s}(t', t)$ of $[W_i]_{(r)}$ and $[W_i]_{(s)}$ is given by

$$\begin{aligned} \Phi_{r,s}(t', t) &= \Pr[W_i]_{(r)} \leq t', [W_i]_{(s)} \leq t \\ &= \sum_{k=s}^{2N+1} \sum_{k'=r}^k \binom{2N+1}{k} \binom{k}{k'} \\ &\quad \times \Phi(t')^{k'} [\Phi(t) - \Phi(t')]^{k-k'} \\ &\quad \times [1 - \Phi(t)]^{2N+1-k} \end{aligned}$$

where r and s are such that $1 \leq r < s \leq 2N + 1$.

Remark. Although Theorem 8 is given in [12] only when $r < s$ and $t' < t$, the result is still valid for $t' \leq t$ and $1 \leq r \leq s \leq 2N + 1$.

Denote by $\tilde{W}_i = W_i - \{X_i\}$ a subwindow of size $2N$, which consists of the same samples as in the windows W_i , except for the center sample X_i .

Now, let us define

$$\begin{aligned} \tilde{\Phi}_r(t) &= \Pr[\tilde{W}_i]_{(r)} \leq t \\ &= \Pr[\text{at least } r \text{ samples in } \tilde{W}_i \text{ are } \leq t] \\ &= \sum_{k=r}^{2N} \binom{2N}{k} \Phi(t)^k (1 - \Phi(t))^{2N-k}. \end{aligned}$$

And for $t' \leq t$, with $1 \leq r \leq s \leq 2N$, let us define

$$\begin{aligned} \tilde{\Phi}_{r,s}(t', t) &= \Pr[\tilde{W}_i]_{(r)} \leq t', [\tilde{W}_i]_{(s)} \leq t \\ &= \sum_{k=s}^{2N} \sum_{k'=r}^k \binom{2N}{k} \binom{k}{k'} \\ &\quad \times \Phi(t')^{k'} [\Phi(t) - \Phi(t')]^{k-k'} \\ &\quad \times [1 - \Phi(t)]^{2N-k}. \end{aligned}$$

It is worth noticing that for $t' \leq t$ and $r = s$ the inequality $[\tilde{W}_i]_{(r)} \leq t'$ implies $[\tilde{W}_i]_{(r)} \leq t$, so that

$$\tilde{\Phi}_{r,r}(t', t) = \Pr[[\tilde{W}_i]_{(r)} \leq t'] = \tilde{\Phi}_r(t'). \quad (10)$$

In order to derive the output distribution function of the relaxed median filter, we need the following lemma and corollary.

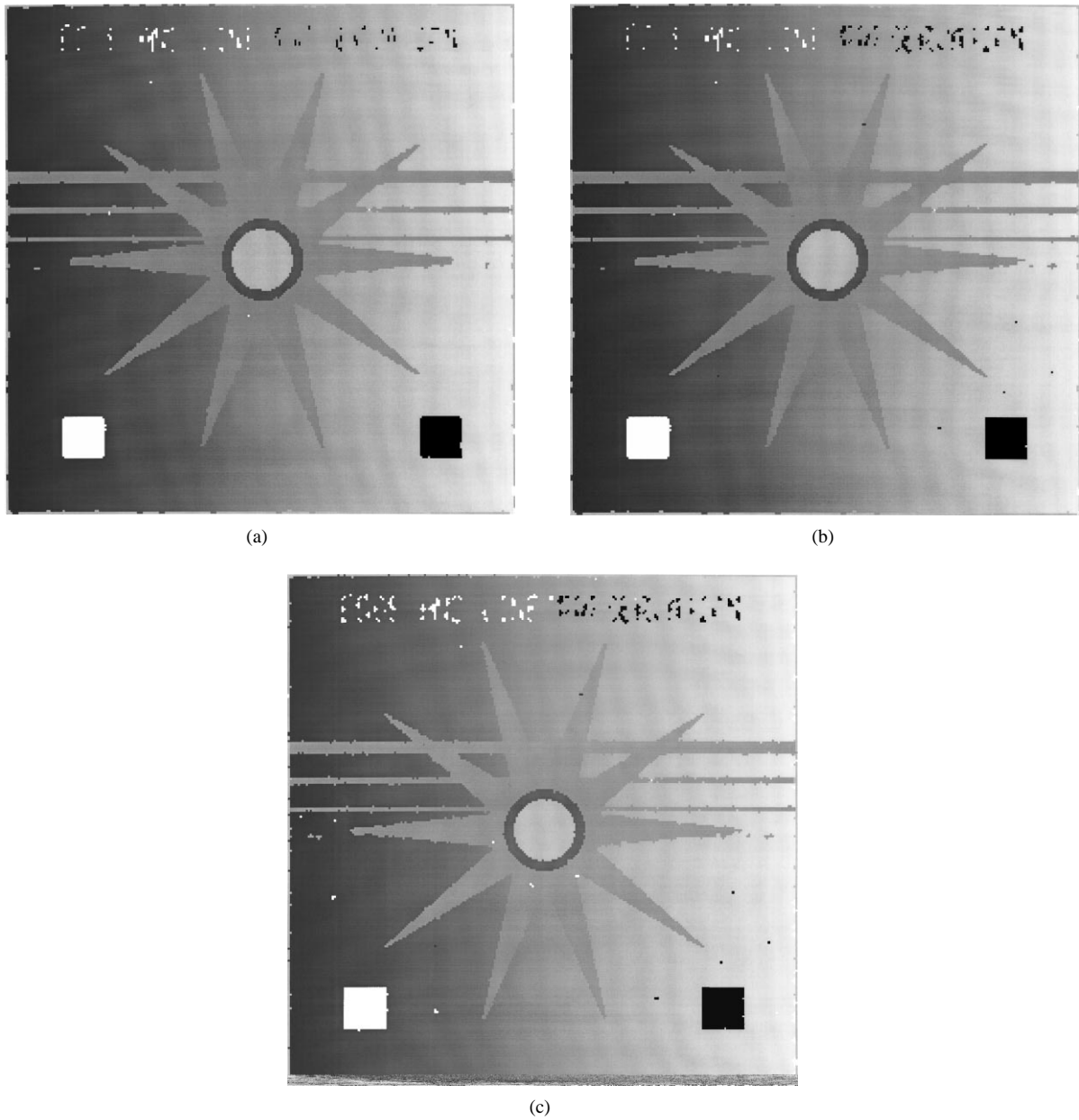


Figure 8. The results of the filtered noisy image in Fig. 7(b) with a 3×3 square window by (a) a standard median filter (SM), (b) a relaxed median filter ($RM_{4,6}$) and (c) a center weighted median filter $CWM(2K + 1 = 3)$.

Lemma 1. For $r \leq s$, let us denote $I_{r,s}(t) = \int_{-\infty}^t \tilde{\Phi}_{r,s}(\tau, t) d\Phi(\tau)$. Then we have

$$I_{r,s}(t) = \sum_{k=s}^{2N} \frac{k+1-r}{k+1} \binom{2N}{k} \Phi(t)^{k+1} (1-\Phi(t))^{2N-k}.$$

Proof:

$$\begin{aligned} I_{r,s}(t) &= \int_{-\infty}^t \Phi_{r,s}(\tau, t) d\Phi(\tau) \\ &= \sum_{k=s}^{2N} \sum_{k'=r}^k \binom{2N}{k} \binom{k}{k'} \int_{-\infty}^t \Phi(\tau)^{k'} \end{aligned}$$



(a)



(b)

Figure 9. (a) Original image. (b) Noisy image corrupted by impulsive noise 15%.

$$\begin{aligned}
 & \times [\Phi(t) - \Phi(\tau)]^{k-k'} [1 - \Phi(t)]^{2N-k} d\Phi(\tau) \\
 & = \sum_{k=s}^{2N} \sum_{k'=r}^k \binom{2N}{k} [1 - \Phi(t)]^{2N-k} \\
 & \quad \times \int_{-\infty}^t \binom{k}{k'} \Phi(\tau)^{k'} [\Phi(t) - \Phi(\tau)]^{k-k'} d\Phi(\tau)
 \end{aligned}$$

By making the substitution $\Phi(\tau) = x \Phi(t)$, and applying the formula

$$\int_0^1 \binom{n}{k} x^k (1-x)^{n-k} dx = \frac{1}{n+1}$$

which is easy to prove, we obtain

$$\begin{aligned}
 I_{r,s}(t) & = \sum_{k=s}^{2N} \sum_{k'=r}^k \binom{2N}{k} \Phi(t)^{k+1} [1 - \Phi(t)]^{2N-k} \\
 & \quad \times \int_0^1 \binom{k}{k'} x^{k'} (1-x)^{k-k'} dx \\
 & = \sum_{k=s}^{2N} \sum_{k'=r}^k \binom{2N}{k} \\
 & \quad \times \Phi(t)^{k+1} (1 - \Phi(t))^{2N-k} \times \frac{1}{k+1} \\
 & = \sum_{k=s}^{2N} \frac{k+1-r}{k+1} \binom{2N}{k} \\
 & \quad \times \Phi(t)^{k+1} (1 - \Phi(t))^{2N-k}.
 \end{aligned}$$

This completes the proof. \square

Corollary 1. Let us denote $J_r(t) = \int_{-\infty}^t \tilde{\Phi}_r(\tau) d\Phi(\tau)$. Then we have

$$\begin{aligned}
 J_r(t) & = \sum_{k=r}^{2N} \frac{k+1-r}{k+1} \binom{2N}{k} \\
 & \quad \times \Phi(t)^{k+1} (1 - \Phi(t))^{2N-k}.
 \end{aligned}$$

Proof: From (10) we have $\tilde{\Phi}_{r,r}(\tau, t) = \tilde{\Phi}_r(\tau)$ for $\tau \leq t$, then we obtain

$$J_r(t) = I_{r,r}(t)$$

which concludes the proof. \square

Proof of Theorem 1: Let $\Psi(t) = \Pr[Y_i \leq t]$ be the output distribution function of the relaxed median filter. To facilitate the computation of $\Psi(t)$, we consider two cases depending on the input X_i .

(a) (See Fig. 11) $X_i \leq t$. In this case, the two mutually exclusive possibilities that the output $Y_i \leq t$ are:

- (a1) $[W_i]_{(m)} \leq t$
- (a2) $[W_i]_{(\ell)} \leq X_i$ and $[W_i]_{(m)} > t$

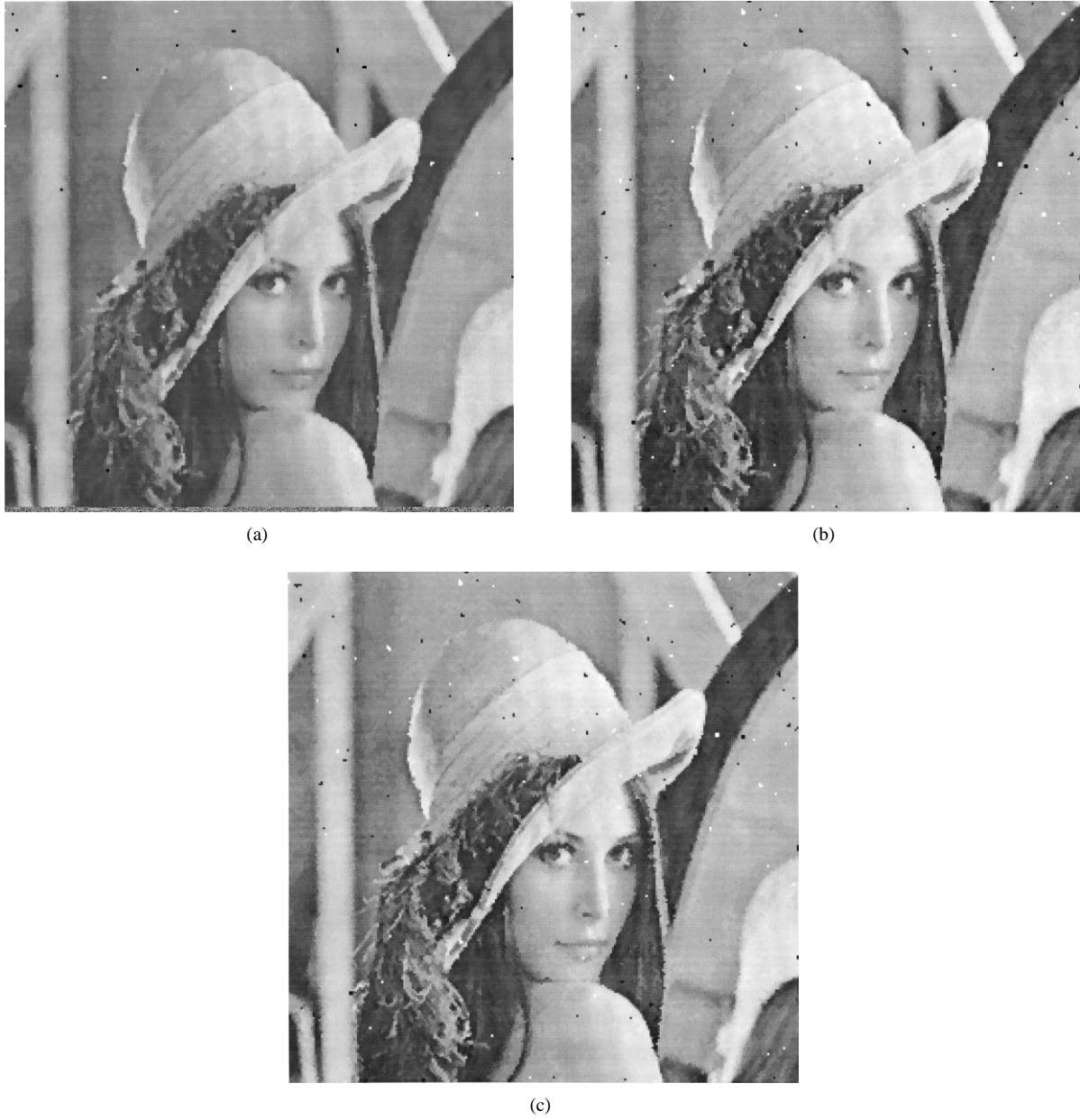


Figure 10. The results of the filtered noisy image in Fig. 9(b) with a 3×3 square window by (a) a standard median filter (SM), (b) a relaxed median filter ($RM_{4,6}$) and (c) a center weighted median filter $CWM(2K + 1 = 3)$.

$$\begin{aligned} & \Pr[Y_i \leq t, X_i \leq t] \\ &= \Pr[X_i \leq t, [W_i]_{(m)} \leq t] \\ &+ \Pr[X_i \leq t, [W_i]_{(m)} > t, [W_i]_{(\ell)} \leq X_i]. \end{aligned}$$

(b) (See Fig. 11) $X_i > t$. In this case, the unique possibility that $Y_i \leq t$ is $X_i > [W_i]_{(u)}$ and $[W_i]_{(m)} \leq t$.

$$\begin{aligned} & \Pr[Y_i \leq t, X_i > t] \\ &= \Pr[[W_i]_{(m)} \leq t, X_i > t, [W_i]_{(u)} < X_i]. \end{aligned}$$

Then,

$$\begin{aligned} \Psi(t) &= \Pr[Y_i \leq t] \\ &= \Pr[Y_i \leq t, X_i \leq t] + \Pr[Y_i \leq t, X_i > t] \\ &= \Psi_1(t) + \Psi_2(t) + \Psi_3(t) \end{aligned}$$

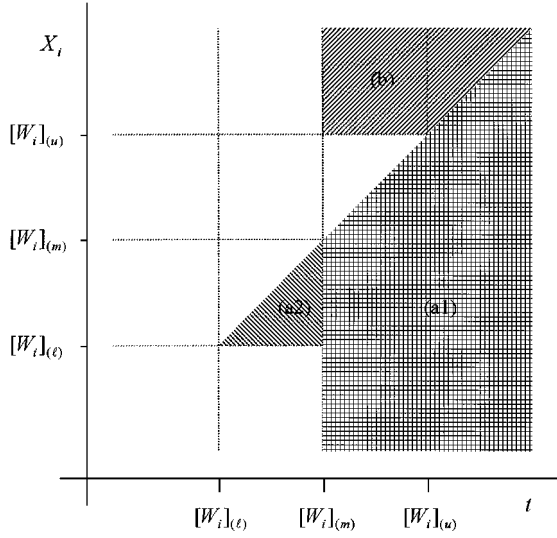


Figure 11. Illustration of the cases (a) and (b). Labelled areas correspond to each case.

where

$$\Psi_1(t) = \Pr[X_i \leq t, [W_i]_{(m)} \leq t]$$

$$\Psi_2(t) = \Pr[X_i \leq t, [W_i]_{(m)} > t, [W_i]_{(l)} \leq X_i]$$

$$\Psi_3(t) = \Pr[[W_i]_{(m)} \leq t, X_i > t, [W_i]_{(u)} < X_i].$$

The explicit expression of $\Psi_1(t)$ is the following

$$\begin{aligned} \Psi_1(t) &= \Pr[[W_i]_{(m)} \leq t/X_i \leq t] \times \Pr[X_i \leq t] \\ &= \Pr[[\tilde{W}_i]_{(m-1)} \leq t] \times \Pr[X_i \leq t] \\ &= \tilde{\Phi}_{m-1}(t)\Phi(t). \end{aligned}$$

Applying the theorem of total probabilities for the continuous case, we have

$$\Psi_2(t) = \int_{-\infty}^t [\tilde{\Phi}_{\ell-1}(\tau) - \tilde{\Phi}_{\ell-1,m-1}(\tau, t)] d\Phi(\tau)$$

In fact,

$$\begin{aligned} \Psi_2(t) &= \int_{-\infty}^t \Pr[[W_i]_{(m)} > t, [W_i]_{(l)} \leq X_i/X_i = \tau] \\ &\quad \times d\Phi(\tau) \\ &= \int_{-\infty}^t \Pr[[\tilde{W}_i]_{(m-1)} > t, [\tilde{W}_i]_{(\ell-1)} \leq \tau] d\Phi(\tau) \end{aligned}$$

$$\begin{aligned} &= \int_{-\infty}^t (\Pr[[\tilde{W}_i]_{(\ell-1)} \leq \tau] - \Pr[[\tilde{W}_i]_{(m-1)} \leq t, \\ &\quad [\tilde{W}_i]_{(\ell-1)} \leq \tau]) d\Phi(\tau) \\ &= \int_{-\infty}^t [\tilde{\Phi}_{\ell-1}(\tau) - \tilde{\Phi}_{\ell-1,m-1}(\tau, t)] d\Phi(\tau). \end{aligned}$$

Similarly, we have

$$\Psi_3(t) = \int_t^{+\infty} \tilde{\Phi}_{m,u}(t, \tau) d\Phi(\tau)$$

In fact,

$$\begin{aligned} \Psi_3(t) &= \int_t^{+\infty} \Pr[[W_i]_{(m)} \leq t, [W_i]_{(u)} < X_i/X_i = \tau] \\ &\quad \times d\Phi(\tau) \\ &= \int_t^{+\infty} \Pr[[\tilde{W}_i]_{(m)} \leq t, [\tilde{W}_i]_{(u)} < \tau] d\Phi(\tau) \\ &= \int_t^{+\infty} \Pr[[\tilde{W}_i]_{(m)} \leq t, [\tilde{W}_i]_{(u)} < \tau] d\Phi(\tau) \\ &= \int_t^{+\infty} \tilde{\Phi}_{m,u}(t, \tau) d\Phi(\tau). \end{aligned}$$

Then, the expression of $\Psi(t)$ is the following

$$\begin{aligned} \Psi(t) &= \tilde{\Phi}_{m-1}(t)\Phi(t) \\ &\quad + \int_{-\infty}^t [\tilde{\Phi}_{\ell-1}(\tau) - \tilde{\Phi}_{\ell-1,m-1}(\tau, t)] d\Phi(\tau) \\ &\quad + \int_t^{+\infty} \tilde{\Phi}_{m,u}(t, \tau) d\Phi(\tau). \end{aligned}$$

Now, we establish the explicit expressions of $\Psi_2(t)$ and $\Psi_3(t)$.

From Lemma 1 and Corollary 1, it holds

$$\begin{aligned} \Psi_2(t) &= J_{\ell-1}(t) - I_{\ell-1,m-1}(t) \\ &= \sum_{k=\ell-1}^{2N} \frac{k-\ell+2}{k+1} \binom{2N}{k} \Phi(t)^{k+1} \\ &\quad \times (1-\Phi(t))^{2N-k} - \sum_{k=m-1}^{2N} \frac{k-\ell+2}{k+1} \\ &\quad \times \binom{2N}{k} \Phi(t)^{k+1} (1-\Phi(t))^{2N-k} \\ &= \sum_{k=\ell-1}^{m-2} \frac{k-\ell+2}{k+1} \binom{2N}{k} \Phi(t)^{k+1} \\ &\quad \times (1-\Phi(t))^{2N-k} \end{aligned}$$

Similarly, we have

$$\begin{aligned} \Psi_3(t) &= \int_t^{+\infty} \tilde{\Phi}_{m,u}(t, \tau) d\Phi(\tau) \\ &= \sum_{k=u}^{2N} \sum_{k'=m}^k \binom{2N}{k} \binom{k}{k'} \int_t^{+\infty} \Phi(t)^{k'} \\ &\quad \times [\Phi(\tau) - \Phi(t)]^{k-k'} \\ &\quad \times [1 - \Phi(\tau)]^{2N-k} d\Phi(\tau) \\ &= \sum_{k=u}^{2N} \sum_{k'=m}^k \binom{2N}{k} \binom{k}{k'} \Phi(t)^{k'} \int_t^{+\infty} [\Phi(\tau) \\ &\quad - \Phi(t)]^{k-k'} [1 - \Phi(\tau)]^{2N-k} d\Phi(\tau) \end{aligned}$$

By making the substitution $\Phi(\tau) = x(1 - \Phi(t)) + \Phi(t)$, we obtain

$$\begin{aligned} \Psi_3(t) &= \sum_{k=u}^{2N} \sum_{k'=m}^k \binom{2N}{k} \binom{k}{k'} \Phi(t)^{k'} [1 - \Phi(t)]^{2N+1-k'} \\ &\quad \times \int_0^1 x^{k-k'} (1-x)^{2N-k} dx \\ &= \sum_{k=u}^{2N} \sum_{k'=m}^k \binom{2N}{k} \binom{k}{k'} \Phi(t)^{k'} (1 - \Phi(t))^{2N+1-k'} \\ &\quad \times \frac{\Gamma(k-k'+1)\Gamma(2N+1-k)}{\Gamma(2N+2-k')} \\ &= \sum_{k=u}^{2N} \sum_{k'=m}^k \frac{(2N)!}{k!(2N-k)!} \times \frac{k!}{k'!(k-k')!} \\ &\quad \times \Phi(t)^{k'} (1 - \Phi(t))^{2N+1-k'} \\ &\quad \times \frac{(k-k')!(2N-k)!}{(2N+1-k')!} \\ &= \sum_{k=u}^{2N} \sum_{k'=m}^k \frac{1}{2N+1-k'} \binom{2N}{k'} \\ &\quad \times \Phi(t)^{k'} (1 - \Phi(t))^{2N+1-k'} \end{aligned}$$

then Eq. (1) follows. \square

Proof of Theorem 5: From Theorem 1, $\Psi_{Y_{ij}}(t)$ can be expressed as

$$\begin{aligned} \Psi_{Y_{ij}}(t) &= \Pr[X_{ij} \leq t] \\ &\quad \times \sum_{k=m-1}^{2N} \Pr[\text{exactly } k \text{ samples in } \tilde{W}_{ij} \text{ are } \leq t] \\ &\quad + \Pr[X_{ij} \leq t] \\ &\quad \times \sum_{k=\ell-1}^{m-2} \frac{k-\ell+2}{k+1} \\ &\quad \times \Pr[\text{exactly } k \text{ samples in } \tilde{W}_{ij} \text{ are } \leq t] \end{aligned}$$

$$\begin{aligned} &+ \Pr[X_{ij} > t] \\ &\quad \times \sum_{k=u}^{2N} \sum_{k'=m}^k \frac{1}{2N+1-k'} \\ &\quad \times \Pr[\text{exactly } k' \text{ samples in } \tilde{W}_{ij} \text{ are } \leq t] \end{aligned} \quad (11)$$

And, from (7), we have

$$\begin{aligned} &\Pr[\text{exactly } k \text{ samples in } \tilde{W}_{ij} \text{ are } \leq t] \\ &= \sum_{n_0=\max\{0, k-(2N-d_{ij})\}}^{\min\{k, d_{ij}\}} \Pr[\text{exactly } n_0 \text{ samples in } A \\ &\quad \text{are } \leq t, \text{ exactly } k-n_0 \\ &\quad \text{samples in } B \text{ are } \leq t] \\ &= \sum_{n_0=\max\{0, k-(2N-d_{ij})\}}^{\min\{k, d_{ij}\}} \binom{d_{ij}}{n_0} \binom{2N-d_{ij}}{k-n_0} \\ &\quad \times \Phi_A(t)^{n_0} (1 - \Phi_A(t))^{d_{ij}-n_0} \times \Phi_B(t)^{k-n_0} \\ &\quad \times (1 - \Phi_B(t))^{2N-d_{ij}-k+n_0} \end{aligned} \quad (12)$$

where d_{ij} is the number of samples with distribution function Φ_A in \tilde{W}_{ij} .

On the other hand, we have $\Pr[X_{ij} \leq t] = \Phi_{ij}(t)$ and $\Pr[X_{ij} > t] = 1 - \Phi_{ij}(t)$.

Then the expression of $\Psi_{Y_{ij}}(t)$ follows directly by combining (11) and (12). \square

References

1. I. Pitas and A.N. Venetsanopoulos, *Nonlinear Digital Filters: Principles and Applications*, Kluwer Academic Publisher, 1990.
2. A.C. Bovik, T.S. Huang, and D.C. Munson, "The effect of median filtering on edge estimation and detection," *IEEE Transactions on Pattern Analysis and Machine Intelligence*, Vol. PAMI-9, No. 2, pp. 181-194, 1987.
3. A. Nieminen, P. Heinonen, and Y. Neuvo, "A new class of detail preserving filters for image processing," *IEEE Transactions on Pattern Analysis and Machine Intelligence*, Vol. PAMI-9, No. 1, pp. 74-90, 1987.
4. G.R. Arce and R.E. Foster, "Detail preserving ranked-order based filters for image processing," *IEEE Transactions on Acoustics, Speech and Signal Processing*, Vol. ASSP-37, No. 1, pp. 83-98, 1989.
5. D.R.K. Brownrigg, "Weighted median filters," *Commun. Assoc. Comput. Machinery*, Vol. 27, pp. 807-818, 1984.
6. O. Yli-Harja, J. Astola, and Y. Neuvo, "Analysis of the properties of median and weighted median filters using threshold logic and stack filter representation," *IEEE Trans. Signal Processing*, Vol. 39, No. 2, pp. 395-409, 1991.
7. S.J. Ko and Y.H. Lee, "Center weighted median filters and their applications to image enhancement," *IEEE Transaction Circuits Systems*, Vol. 38, No. 9, pp. 984-993, 1991.

8. T. Song, M. Gabbouj, and Y. Neuvo, "Center weighted median filters: Some properties and applications in image processing," *Signal Processing*, Vol. 35, No. 3, pp. 213–229, 1994.
9. R. Yang, L. Yin, M. Gabbouj, J. Astola, and Y. Neuvo "Optimal weighted median filters under structural constraints," *IEEE Trans. Signal Processing*, Vol. 43, No. 3, pp. 591–604, 1995.
10. P.D. Wendt, E.J. Coyle, and N.C. Gallagher, "Stack filters," *IEEE Transactions Acoustics, Speech and Signal Processing*, Vol. ASSP-34, No. 4, pp. 898–911, 1986.
11. E.J. Coyle, J.-H. Lin, and M. Gabbouj, "Optimal stack filtering and the estimation and structural approaches to image processing," *IEEE Transactions on Acoustics, Speech and Signal Processing*, Vol. ASSP-37, No. 12, pp. 2037–2066, 1989.
12. H.A. David, *Order Statistics*, John Wiley, 1981.
13. J. Andrew Bangham, "Properties of a series of nested median filters, namely the data sieve," *IEEE Trans. Signal Processing*, Vol. 41, No. 1, pp. 31–42, 1993.
14. R.C. Hardie and K.E. Barner, "Rank conditioned rank selection filters for signal processing," *IEEE Trans. Signal Processing*, Vol. 3, No. 2, pp. 192–206, 1994.



Abdessamad Ben Hamza received the licentiate degree in Mathematics in 1993 from the University of Tetuan, Morocco, and the Ph.D. degree in Applied Mathematics in 1997 from the University of Granada, Spain. His research interests are nonlinear image processing and information theory.



Pedro Luque Escamilla was born in Granada, Spain in 1968. He received his B.Sc. degree in Physics from the Complutense Univer-

sity of Madrid, Spain, and his Ph.D. degree in Applied Physics in 1996 from the University of Granada, Spain. He is adscribed to the Department of Mineral and Mechanical Engineering, University of Jaen, Spain, since 1995. His present research interests include edge detection for fisheries, and other applications of image processing to medical and physical (fluid mechanics) topics.



José Martínez Aroza received his B.Sc. degree in Mathematics in 1979 from the University of Granada, Spain. From 1979 to 1987 he was a professor at the University of Almería, Spain. He received the Ph.D. degree in Applied Mathematics in 1990 from the University of Granada, Spain. He is Associate Professor at the Department of Applied Mathematics, University of Granada, Spain. His research interests lie on the field of digital image processing, more specifically on noise filtering and segmentation of homogeneous as well as textured regions.



Ramón Román Roldán is Professor of Applied Physics at the University of Granada, Spain. He is currently researching in two inter-related subjects, both based on the use of an information-theoretic measure, the Jensen-Shannon divergence: entropic edge detection in digital images, and complexity analysis in DNA sequences through entropic segmentation.